Influence of Fiber Treatment on the Performance of Sisal–Polypropylene Composites

Smita Mohanty,[1] Sushil K. Verma,[2] Sanjay K. Nayak,[1] Sudhansu S. Tripathy[3]

[1]*Central Institute of Plastics Engineering and Technology, Bhubaneswar, India*
[2]*Corporate Office, Central Institute of Plastics Engineering and Technology, Guindy, Chennai, India*
[3]*The Uranium (Society for the Advancement of Education and Research in Chemical Sciences), Friends Colony, Cuttack, India*

Received 19 February 2004; accepted 7 July 2004
DOI 10.1002/app.21161
Published online in Wiley InterScience (www.interscience.wiley.com).

ABSTRACT: This article concerns the effectiveness of MAPP as a coupling agent in sisal–polypropylene composites. The fiber loading, MAPP concentration, and fiber treatment time influenced the mechanical properties of the composites. It was observed that the composites prepared at 21 volume percent of fibers with 1% MAPP concentration exhibits optimum mechanical strength. SEM investigations confirmed that the increase in properties is caused by improved fiber-matrix adhesion. The viscoelastic properties of the treated and untreated composites were also studied. From the storage modulus versus temperature plots, an increase in the magnitude of the peaks was observed with the addition of MAPP and fiber reinforcement, thus showing an improvement in stiffness of the treated composites. The damping properties of the composites, however, decreased with the addition of the fibers and MAPP. The thermal properties of the composites were analyzed through DSC and TGA measurements. © 2004 Wiley Periodicals, Inc. J Appl Polym Sci 94: 1336–1345, 2004

Key words: fibers; mechanical properties; PP; viscoelastic properties; TGA

INTRODUCTION

Short fiber reinforced composites of thermoplastic materials have emerged as a major class of structural materials in the fields of aerospace, automotives, construction, textiles, etc. These materials offer a unique combination of high strength to weight ratio, better dimensional stability, and heat and environmental resistance that are either comparable to or better than many conventional materials. Further, the need for eco-friendly biodegradable plastic composites has completely changed the global scenario.

Lignocellulosic natural fibers, such as jute, sisal, coir, etc., have gained substantial importance as reinforcements in polymer matrix composites.[1–8] Easy availability, low cost and density, high specific properties, nonabrasive nature, and biodegradability characteristics are the primary benefits in the broad use of these fibers commercially. Despite the advantages, use of natural fiber filled composites has been restricted due to its inherent high moisture absorption capacity, thermal instability during processing, poor wettability, and poor adhesion towards commercial synthetic resins. These factors further lead to ineffective interface with the polymer matrix, resulting in poor composite properties. An extensive literature survey reveals that many attempts have been made in modifying the interfacial characteristics between the fiber and matrix phases[9–13] to overcome the limitations in the broad use of these fibers. Various surface modification techniques, like mercerization, cyanoethylation, acetylation, coupling agent treatment, gamma ray irradiation, etc., have been reported to improve the resin pick up or wettability during composite fabrication.

In the present investigation, our main objective is to determine the suitability of sisal fibers as reinforcement in the PP matrix. Among the various natural fibers, sisal fiber possesses moderately high specific strength and stiffness. However, its high lignin content leads to a greater degree of water absorption and, hence, poor adhesion with the hydrophobic thermoplastic matrix. Maleic anhydride grafted PP (MAPP) has been used as the coupling agent to improve the interfacial bonding between the fibers and PP matrix. A systematic study of the mechanical properties of the composites as a function of fiber loading, MAPP concentration, and fiber treatment time has been made to obtain maximum mechanical strength. The composite samples were subjected to DMA measurements to evaluate the glass transition temperature (T_g), stiffness, and damping properties, under periodic stress. Fractured surface morphologies of the hybrid composites were observed with scanning electron microscope to investigate the fiber matrix interface. Thermal sta-

Correspondence to: S. K. Nayak (cipet_bbsr@sify.com).

© 2004 Wiley Periodicals, Inc.

TABLE I
Physical and Mechanical Properties of Sisal Fiber

Properties	
Density	1.45
Cellulose content (%)	85–88
Lignin content (%)	4–5
Tensile strength (MPa)	575.43
Youngs modulus(MPa)	149.90
Elongation (%)	3.98
Stiffness (GPa)	9–12.58

bility of the composites was studied from TGA and DSC thermograms. Water absorption and aging behavior were also investigated to evaluate the extent of mechanical degradation in the composites.

EXPERIMENTAL

Materials

Random copolymer of polypropylene (R120MK) with a density of 0.91 g/cc and melt flow index of 12 g/10 min, obtained from M/s Reliance Industries Ltd., Mumbai, India, was used as the base polymer matrix.

Sisal fibers having an average fiber diameter of 40 μm, obtained from Keonjhar (Orissa, India), were used as reinforcing agent. The physical and mechanical properties of the fibers are listed in Table I.

MAPP, supplied by M/s Eastman Chemicals Ltd. Germany, under the trade name Epolene G-3015, having $<$ 1.0 wt % maleic anhydride, with M_w 47,000 and acid number 15, was used as coupling agent.

Fiber treatment

The fibers, scoured in hot detergent solution (2%) at 70°C for 1 h to remove dirt and core material, followed by washing with distilled water, were dried in a vacuum oven at 70°C. The dried fibers were cut to the desired length of 6 mm, using an electronic fiber cutting machine. These detergent washed untreated fibers were then immersed in MAPP solution (in toluene) at 100°C at various concentration (0.3, 0.5, and 1% w/v) and time periods (3, 5, and 10 min) to obtain treated fibers.

Preparation of composite samples

The composite samples were prepared in two stages. In the first stage, PP and untreated fibers at various volume percent of fiber loading (6.8, 10.3, 21, and 31%) were melt mixed at 190°C in Torque Rheocord-9000 (Haake, Germany), using sigma roller blades and a mixing chamber of 69 cm^3 volumetric capacity. The mixing was carried out for 10 min at a rotor speed of 25 rpm. In the second stage, MAPP treated fibers were mixed with PP at the same optimized condition of 190°C and 25 rpm rotor speed.

Subsequently, these melt mixes (treated as well as untreated) were brought to room temperature and compression molded using a 100T press (Delta Malikson Pressman, India) at 170°C to produce sheets of 3 $\pm$ 0.1mm thickness.

A contour cut-copy milling machine; 6490 (Ceast, Italy), was used for the preparation of test specimens from the sheets as per ASTM-D 638, 790, 256, and 570, using calibrated templates.

Physico-mechanical properties

Tensile strength

Specimens of virgin PP and untreated and treated composites having dimensions 165 $\times$ 13 $\times$ 3 mm were subjected to tensile tests as per ASTM-D-638, using Universal Testing Machine (UTM), LR-100K (Lloyd Instruments Ltd. U.K.) at 100 mm/min crosshead speed and 50 mm gauge length.

Flexural strength

Specimens of virgin PP and untreated and treated sisal–PP composites having dimensions 80 $\times$ 12.7 $\times$ 3 mm were taken for flexural test, under three point bending, using the same Universal Testing Machine (UTM), in accordance with ASTM-D 790, at a crosshead speed of 1.3 mm/min and a span length of 50 mm.

Impact strength

Similarly, izod impact strength was determined from the specimens having dimensions 63.5 $\times$ 12.7 $\times$ 3 mm with a "V" notch depth of 2.54 mm and notch angle of 45°, as per ASTM-D-256, using Impactometer 6545 (Ceast, Italy).

Water absorption

The extent of water absorption of both untreated and treated composites was determined as per ASTM-D-570. The outer edges of the specimens (50 mm diameter) were sealed with epoxy, conditioned at 50°C for 24 h, and the final conditioned weight (w_1) was determined. Subsequently, these conditioned specimens were immersed in distilled water for 24 h, dried, and its final immersed weight (w_2) was measured. Since there were no soluble components, the reconditioned weight (w_3) of the immersed sample was ignored. Percentage of water uptake (WA) was calculated as follows.

$$WA = (w_2 - w_1)/w_1 \times 100\% \quad (1)$$

Further, to evaluate the extent of hydrothermal degradation, tensile specimens of untreated and treated composites were immersed in distilled water for different time periods of 10, 20, 30, and 50 h, respectively. Corresponding tensile strength as a function of immersion time was determined as per ASTM-D-638 using the same Universal Testing Machine.

Five replicate specimens were tested at 23°C and 55% RH for each of the above tests, and the mean values were reported.

Thermal properties

Thermogravimetric analysis (TGA)

Sisal fiber, virgin PP, and untreated and treated composites were subjected to TGA using Perkin–Elmer Pyris-1, USA equipment. Samples of $\leq$ 5 mg weight were heated at the rate of 20°C per minute in nitrogen atmosphere from 30 to 700°C, and corresponding weight loss with temperature was recorded.

Differential scanning calorimetry (DSC)

Virgin PP along with the untreated and treated sisal–PP composite samples were subjected to DSC analysis using Perkin–Elmer, Pyris-6- (U.S.A) equipment. Samples of $\leq$ 5 mg weight were heated from 40 to 200°C at the rate of 10°C/min under nitrogen flow. Corresponding melting points, heats of fusion, and degree of crystallinity of different samples were determined from the DSC thermograms.

Dynamic mechanical properties

Viscoelastic properties, such as storage modulus (E'), loss modulus (E''), and mechanical damping parameter (tanδ), as a function of temperature were measured in a Dynamic Mechanical Thermal Analyzer (VA 4000, Germany). The measurements were carried out in tensile mode using a rectangular specimen of dimensions $27.4 \times 3.1 \times 3$ mm over a temperature range of –100 to 150°C, at a heating rate of 3°C/min, under nitrogen flow. The samples were scanned at a fixed frequency of 10 Hz, with a static strain of 0.2% and dynamic strain of 0.1%.

Scanning electron microscopy (SEM) analysis

The tensile fractured surfaces of the composites were taken for morphological study using SEM (JEOL-JSM 5800, Japan). The samples were gold sputtered (50 nm thickness) and dried for half an hour in vacuum at 100°C prior to study.

TABLE II
Effect of Fiber Loading on Mechanical Strength

Fiber vol %	Tensile strength (MPa)	Flexural strength (MPa)	Impact strength (J/m)
PP (virgin)	17.80	19.60	23.25
6.8	24.17	34.83	40.50
10.3	26.11	46.35	46.10
21.0	29.25	48.96	51.79
31.0	23.21	43.41	39.83

Fourier transformation infrared spectroscopy (FTIR)

FTIR spectra of MAPP copolymer and untreated and treated sisal fibers were recorded using Perkin–Elmer 1720X (U.K.) spectrometer. Each spectrum was obtained by coadding 64 consecutive scans with a resolution of 4 cm^{-1} within the range of 400 to 4000 cm^{-1}. The samples were studied using the KBr pellet method.

RESULTS AND DISCUSSION

Mechanical properties

Effect of fiber loading

The mechanical properties of virgin PP and untreated sisal–PP composites, as a function of fiber loading, are presented in Table II.

It is evident that the mechanical properties of the composites increased linearly with the increase in fiber loading from 6.8 to 21%. Tensile strength increased to about 64%, whereas flexural and impact strengths increased to about 119 and 123%, respectively, as compared with the virgin polymer. This behavior is primarily attributed to the reinforcing effect of the fibers, leading to a uniform stress distribution from a continuous polymer matrix to a dispersed fiber phase.

However, it was observed that with the increase in fiber loading from 21 to 31 volume percent, all the mechanical properties deteriorated. A decrease of nearly 26, 13.2, and 30% in tensile, flexural, and impact strengths, respectively, was noticed. This decrease in the mechanical properties at high fiber loading is probably due to incompatibility of the fibers within the matrix, which promoted microcrack formation at the interface as well as nonuniform stress transfer due to fiber agglomeration in the matrix.[14,15]

Effect of MAPP treatment

Sisal fibers are hydrophilic in nature, mainly as a consequence of their chemical structures. The hydroxyl and carboxylic acid groups present in the fibers are the active sites for absorption of water. This leads to weak interfacial bonding, with consequent prob-

TABLE III
Effect of Concentration of MAPP on Mechanical Strength of 21 Vol % Fiber Filled PP

MAPP conc. (in % age)	Tensile strength (MPa)	Flexural strength (MPa)	Impact strength (J/m)
0.3	32.35	50.13	52.45
0.5	35.44	52.44	57.16
1.0	43.66	62.42	68.66
2.0	34.55	51.16	55.30

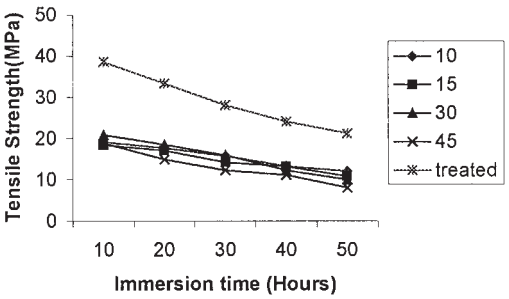

Figure 1 Variation of tensile strength with water absorption.

lems such as poor stress transfer, small void spaces, and debonding in the resulting composites. Therefore, to reduce the surface hydrophilicity, the fiber surface is treated with MAPP. The anhydride rings of MAPP covalently link with the hydroxyl groups of the fibers to form ester linkage. Furthermore, the PP long chains of MAPP being compatible with the virgin matrix, lowers the surface tension of the fiber and increases its wettability within the matrix. As implied from the test results reported in Table III, the MAPP treated composites at 21% fiber loading exhibited better mechanical properties in comparison to the untreated composites at the same volume percent of fiber content. The composite prepared using 1% MAPP concentration showed optimum mechanical strength. Tensile strength increased by 49%, while flexural and impact strengths increased by 30 and 58%, respectively, as compared with 30% for the untreated composite. This increase in the mechanical strength possibly occurred due to improved interfacial adhesion between the fibers and the matrix, which results in efficient stress transfer from the matrix to the fiber. A similar phenomenon has also been investigated by a number of workers.[16–18] The formation of ester linkage between the anhydride group of MAPP and hydroxyl groups of the fiber has been reported by Gattenholm et al.[19] through IR and ESCA analysis. However, with further increase in MAPP concentration from 1 to 2%, there was a drop in the mechanical strength of the composites. This behavior is attributed to migration of excess MAPP, causing self-entanglement among themselves and with the PP molecules, resulting in slippage.[20]

Effect of fiber treatment time

The variation of mechanical strength as a function of fiber treatment time is presented in Table IV.

From the table, it is evident that the mechanical properties of the composites increased with the increase in fiber treatment time from 3 to 5 min. Tensile strength increased to about 10.5%, with flexural and impact strengths increasing to about 21 and 45%, respectively. The enhanced properties due to the coupling effect of MAPP is mainly based on reduction in fiber pullouts and less fiber matrix debonding, which subsequently leads to micropores at the interface.[21] Similar investigations have been reported by Mieck et al.[22]and Gassan et al.[18] However, a longer treatment time of 10 min resulted in deterioration in the mechanical strength of the composites. This may be due to cellulosic chain scission at high temperature, resulting in loss of strength of the fibers.

Water absorption

Water diffuses through the composites by capillary action along the fiber matrix interface, followed by diffusion from the interface into the bulk resin.[15] This results in the development of shear stress at the interface, thereby leading to debonding, delamination, and loss of structural integrity in the composites.[23] A relative change in the tensile strength of untreated and treated composites with water absorption is enumerated in Figure 1. It is evident that the tensile strength of the composites decreased with the increase in fiber loading and

TABLE IV
Effect of Time Period of Treatment on Mechanical Strength

Treatment time (mins.)	Tensile strength (MPa)	Flexural strength (MPa)	Impact strength (J/m)
Untreated	29.25	48.96	51.79
3	39.69	52.70	56.21
5	43.84	63.66	81.57
10	41.59	53.17	64.71

TABLE V
Water Absorption of Treated and Untreated Sisal–PP Composites

Fiber vol (%)	Conditioned weight (w_1)	Immersed weight (w_2)
6.8	6.63	6.79
10.3	6.75	7.08
21.0	6.93	7.88
31.0	6.96	8.49
21 (MAPP treated)	6.89	7.47

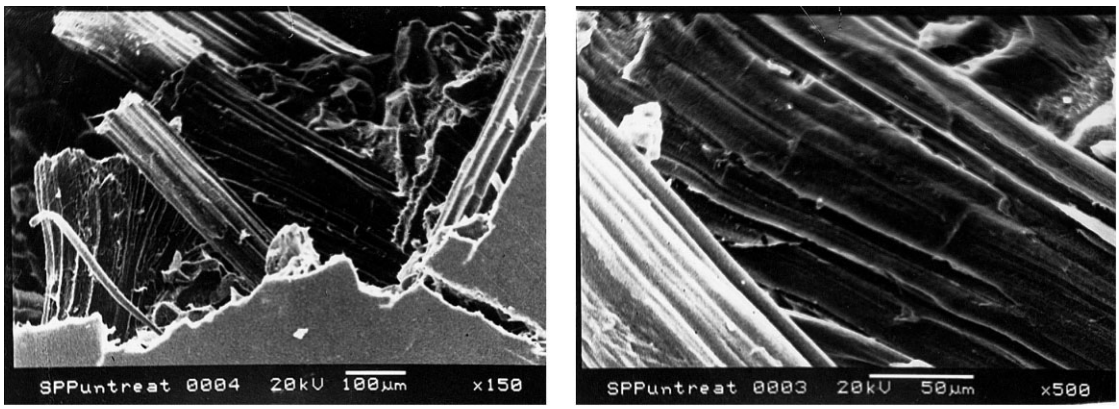

(A) (B)

Figure 2 SEM micrographs of untreated samples.

immersion time. This is because water molecules tend to plasticize the system, subsequently disturbing the fiber matrix interface. The untreated composites at 31% fiber loading showed the maximum tendency of water uptake, and hence a greater reduction in strength, which may be primarily attributed to the increase in the cellulose content with the increase in the fiber loading. The extent of water absorption in the composites is presented in Table V. However, the MAPP treated composites at 21% fiber loading exhibited a fairly higher magnitude of tensile strength and a reduced water uptake, in comparison to the untreated composite under similar conditions. This phenomenon is probably due to efficient wettability of the fibers within the matrix that reduced water accumulation in the interfacial voids.

The treated composites (21 volume percent of fibers, treated for 5 min at 1% MAPP concentration) and the untreated composite (21% fiber loading) were taken for further characterization studies.

Scanning electron microscopy analysis

The effective compatibility of sisal fiber with PP while using MAPP as a coupling agent is depicted in scanning electron micrographs of tensile fractured composites in Figures 2a, 2b, 3a, and 3b, respectively. In the case of untreated composites (Figs. 2a and 2b), well defined holes of pulled out fibers could be observed. This is mainly due to weak interfacial interactions between the fibers and the matrix. On the contrary, with 1% MAPP treatment, the scanning electron micrographs manifested improved adhesion. The fiber surface is well impregnated by a thin polymer layer, which reduced fiber pullouts and the gaps between the matrix and the fibers. In the same case, some gaps between the matrix and fibers were still noticed while the rest of the fibers seemed to be firmly bonded with the matrix. This is probably due to displacement of the fibers by the tensile forces.

Fourier transformation infrared spectroscopy

The existence and type of interfacial bonds in the system was further studied using Fourier transformation infrared spectroscopy. Experiments were carried out on the untreated and treated sisal fibers and compared with pure MAPP (Fig. 4). In the spectrum of the copolymer (Fig. 4c), apart from the PP peaks, charac-

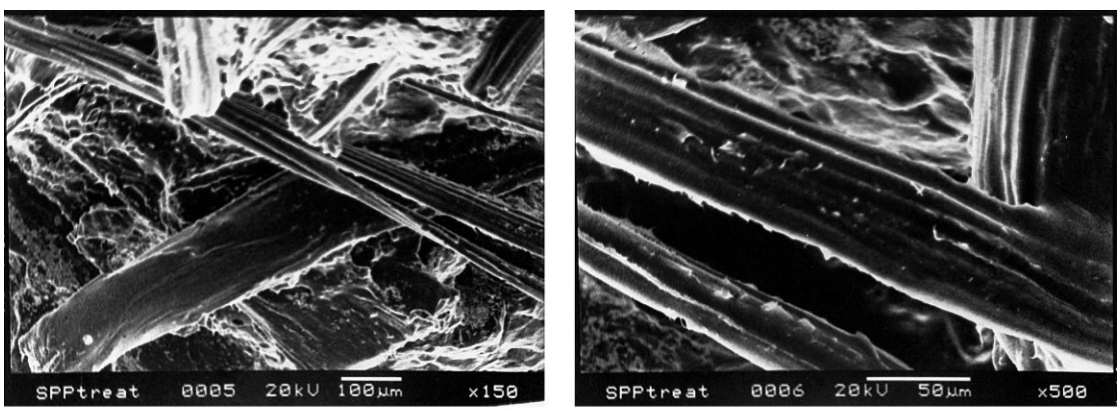

(A) (B)

Figure 3 SEM micrographs of MAPP treated samples.

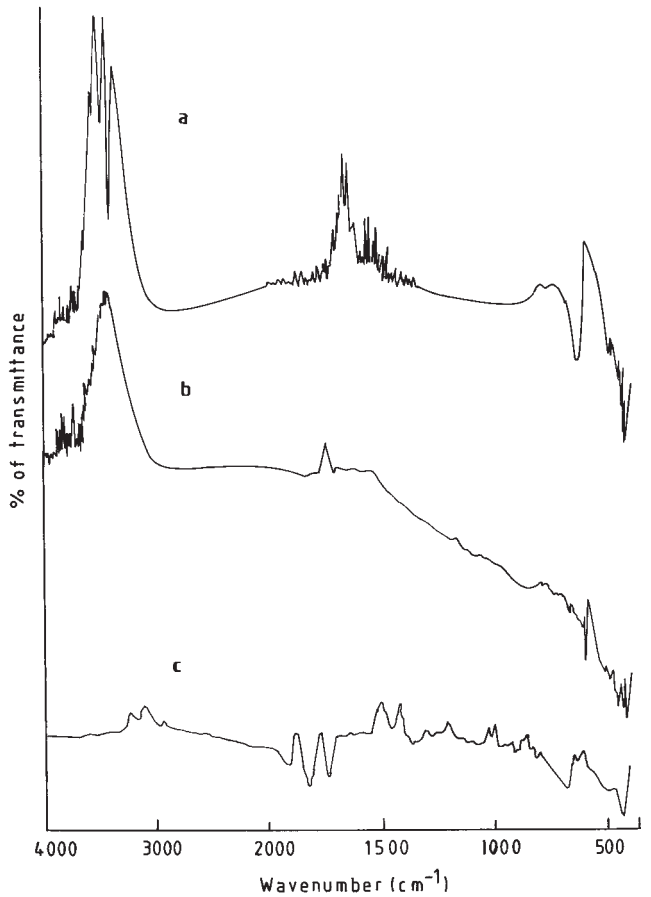

Figure 4 FTIR spectra of (a) untreated and (b) treated sisal fiber and (c) MAPP copolymer.

teristic peaks of the maleic anhydride group at 1865, 1788, and 1717 cm^{-1} were observed. However, in the treated sisal fiber (Fig. 4b), only an ester group was detected located around 1585cm^{-1}, which further substantiates the covalent linkage between the maleic anhydride group of MAPP and hydroxyl groups of the fibers.

The FTIR spectra of untreated sisal fibers (Fig. 4a) showed maximum water absorption in the regions from 400 to 3000 cm^{-1}. On the other hand, the spectrum of MAPP treated fibers manifested substantially reduced water absorption, with a decreased peak area and intensity.

Thermal properties

Differential scanning calorimetry (DSC) analysis

The treated and untreated composites along with virgin PP were subjected to DSC analysis at a heating rate of 10°C/min from 40 to 200°C under nitrogen atmosphere.

From Figures 5a and 5b, it is evident that the DSC melting peak in the untreated composites exhibited a higher melting temperature (163°C) in comparison to the virgin matrix (147°C). This may be due to the higher secondary forces arising from the polar groups present in the sisal fibers. However, the reduction of heat of fusion ΔH in these composites indicates that the crystallinity of the virgin matrix decreases with the incorporation of the fibers. This might be attributed to the presence of the same polar groups that restrict the

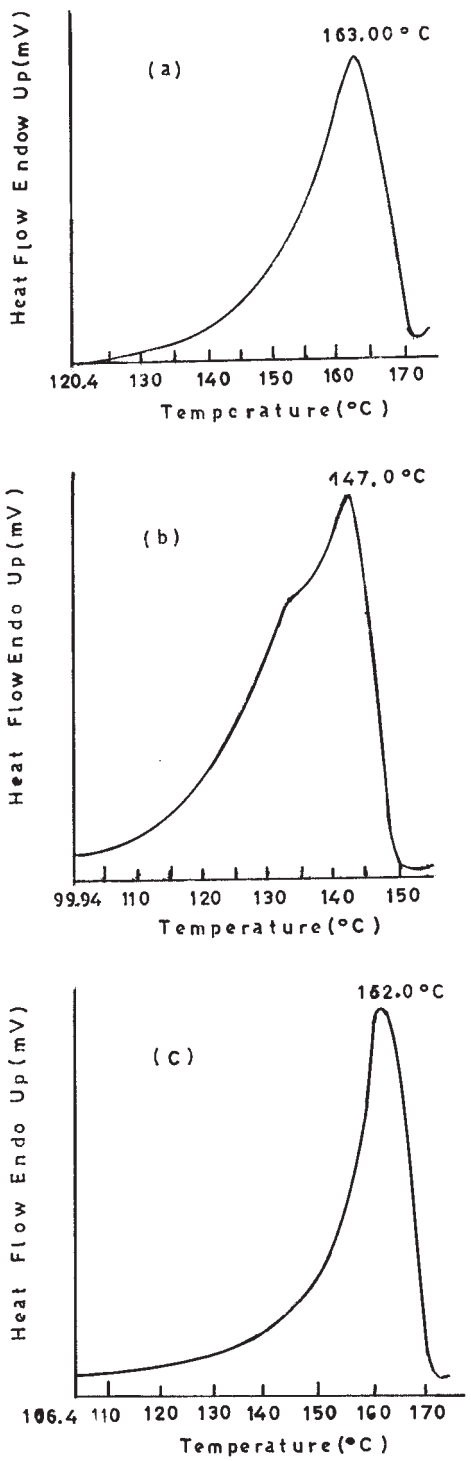

Figure 5 DSC thermogram of (a) untreated sisal–PP composite, (b) PP virgin, and (c) treated sisal–PP composite.

TABLE VI
Melting Properties of Virgin PP and Untreated and Treated Sisal–PP Composites

Sample	Tm (onset °C)	ΔH (J/g)	X_c
PP (virgin)	129.82	65.95	27.40
Sisal–PP (untreated)	151.72	62.05	25.80
Sisal–PP (treated)	152.63	75.84	31.50

large scale segmental motions needed for extended crystal growth and prevent the high melting composites from achieving high levels of crystallinity. The degree of crystallinity X_c of the virgin matrix and untreated and treated sisal–PP composites can be determined from the heat of fusion normalized to that of the PP homopolymer according to the following equation as reported by Xie et al.[24]:

$$X_c = (\Delta Hm/\Delta H^*) \times 100\% \quad (2)$$

where ΔHm and ΔH^* are the melting heats of the composites and PP with 100% crystallinity. According to the literature, ΔH^* of 100% crystalline PP is estimated to be 245 J/g. The results tabulated in Table V further confirm our assumptions.

Figure 5c represents the DSC melting peak of the MAPP treated composites, which show a marginal depression in the melting point (162°C). This means that in the MAPP treated composites, there are some interactions between PP and MAPP. Moreover, there are also some interactions between the fibers and MAPP. Thus, the compatibility between the fibers and the matrix is increased with the addition of MAPP, which further contributes to an efficient fiber–matrix adhesion. The heats of fusion data and degree of crystallinity X_c data in Table VI also reveal high levels of crystallinity with the addition of MAPP. This fact can be further corroborated with an increase in the mechanical strength of the treated composites.

Thermo gravimetric analysis

The thermogravimetric and differential thermogravimetric curves of virgin PP, sisal fiber, and untreated and treated composites are presented in Figure 6. In the case of sisal fiber (Fig. 6b), the initial peak between 30 to 150°C indicates removal of moisture from the fiber with a temperature maximum of 57.7°C. The percentage of weight loss at this stage is about 6%. At 200°C and thereafter, the decomposition of the fiber takes place at a faster rate. As revealed from the DTG curve (Fig. 7b), the primary decomposition temperature occurs at 380°C corresponding to a weight loss of about 72%. This is possibly due to thermal cleavage of the glycosidic linkage by transglycosylation and scission of C-O and C-C bonds and loss of α cellulose from the fiber. A charred residue of carbonaceous products[25] was obtained above 592.1°C. The loss of hemicellulose from the sisal fiber occurs at 307.2°C, as revealed from the DTG curve. It is evident that the major decomposition range of hemicellulose and α cellulose lies between 207 to 592.1°C.

The TGA/DTG curves of virgin PP, represented in Figures 6a and 7a, respectively, indicate that the decomposition takes place at a temperature of 390°C, and nearly 100% decomposition occurred at 490°C. This temperature range was comparatively higher than those of the fibers. Step analysis of the PP-TG scan reveals 0% weight loss from 30 to 150°C. On the contrary, TGA/DTG curves reveal a comparatively higher thermal stability of the PP matrix with the incorporation of fibers. The minor decomposition peak observed at 410 and 408°C in the untreated (Fig. 6c) and treated (Fig. 6d) composites corresponds to degradation of PP. The major degradation at 510°C as revealed from the DTG curve (Fig. 7c and 7d) is possibly due to degradation of dehydrocellulose. Comparing the weight loss at 400°C, approximately a weight loss of about 30% for the untreated fibers and 26.2% for the treated composite was noted. This shows a marginally higher thermal stability in the MAPP treated composite, thus confirming the presence of intermolecular bonding between the fibers and the matrix due to the formation of ester linkage.

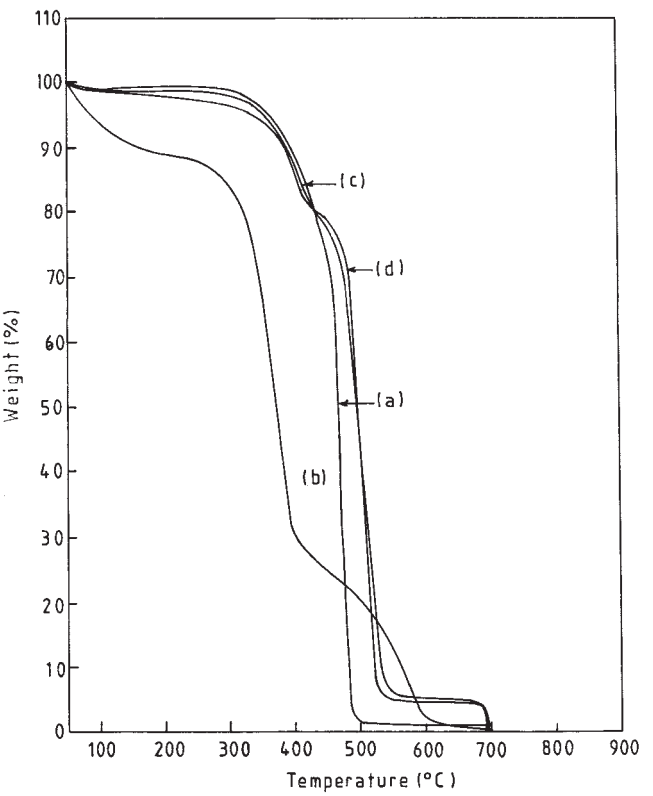

Figure 6 TGA of (a) virgin PP, (b) untreated sisal–PP composite, and (c) treated sisal–PP composite.

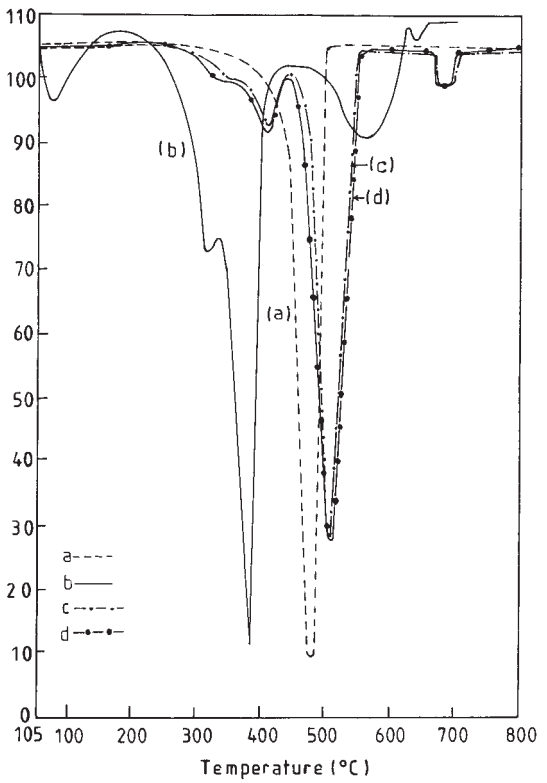

Figure 7 DTG of (a) virgin PP, (b) untreated sisal–PP composite, and (c) treated sisal–PP composite.

At a temperature of 550°C, PP got completely decomposed, whereas in the case of sisal fibers and filled composites, a residue of carbonaceous products was observed.[26]

Dynamic mechanical properties

Storage modulus (E′)

The elastic component, E′, is a measure of load bearing capacity of a material and is analogous to flexural modulus E, determined in accordance with ASTM-D 790.[27] A comparative account of E′ and E of virgin PP and untreated and treated composites, evaluated at 30°C, is presented in Table VII. The variation of E′ as a function of temperature for different samples is graphically represented in Figure 8. It is evident that addition of untreated as well as treated fibers increases the modulus of the virgin matrix. The data reported in Table VI revealed that E′ and E in the untreated composites increased to the tune of 23 and 72%, respectively, as compared with PP. This behavior is primarily attributed to the reinforcing effect imparted by the fibers that allowed a greater degree of stress transfer at the interface.[28] However, at low temperatures between −80°C to −25°C, E′ curves of PP and untreated composites displayed nearly the same magnitudes, indicating that the fibers do not contribute much towards imparting stiffness to the material in these regions. Similar investigations have been reported by George et al.[25] for PALF fiber reinforced LLDPE composites.

A comparatively higher magnitude of E′ was obtained with the MAPP treated composites over the entire range of temperature, thus showing improved interaction between the fibers and the matrix. In all the samples, the storage modulus decreased with the increase in temperature and exhibited a significant fall between −20 to 50°C, which probably referred to the glass transition region of the matrix. In the case of the virgin matrix, E′ drops steeply on increasing the temperature due to increased segmental mobility of the polymer chains. Conversely, with the fiber filled composites, the drop of the matrix modulus was compensated by the interactions caused by the presence of the fibers. This further confirms an increase in the thermal stability of the matrix polymer with the addition of sisal fibers.

TABLE VII
Flexural and Storage Modulus of Virgin PP Composites

Sample	Flexural modulus (MPa)	Storage modulus (MPa)
PP (virgin)	1782	7.69E + 08
Sisal–PP (untreated)	2188	1.32E + 09
Sisal–PP (treated)	3134	1.68E + 09

Loss modulus (E″)

PP shows three relaxation peaks at −80°C (γ), 8°C (β), and 100°C (α), respectively. The temperature of β relaxation maximum corresponds to the Tg of the matrix, while the α relaxation peak is related to the slip mechanism in the crystallites. The γ relaxation peak is due to the motion of small chain groups like methyl and methylene.[8] In the present study, α and β relaxation phenomenon of virgin PP and untreated and

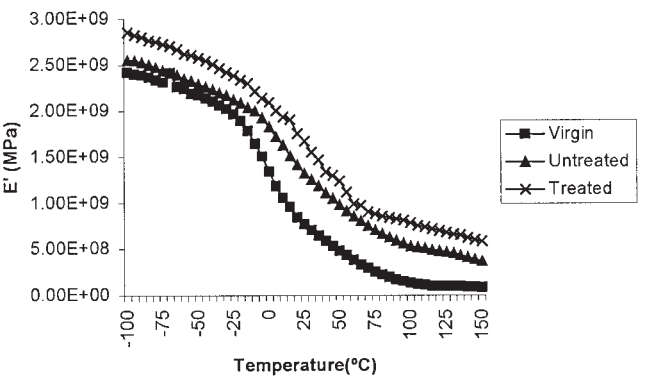

Figure 8 Variation of storage modulus of virgin PP and untreated and treated sisal–PP composites as a function of temperature.

treated composites has been investigated from loss modulus (E″ curves) represented in Figure 9. In the case of virgin PP, the maxima of the peak at a temperature of –5°C is associated with the T*g* of the matrix, whereas the high temperature peak at 55°C is probably related to the onset of melting of PP crystallites. In the composites prepared from 21% untreated fibers, the primary transition peak, that is, T_g, shifted to a comparatively higher temperature (5°C). This is primarily attributed to immobilization of polymer molecules near the surface of sisal fibers due to molecular interactions caused by the latter. The E″ values corresponding to the T_g in the untreated composites (8.39E + 07 MPa) also increased considerably, to about 30%, in comparison to virgin PP (6.48E + 07 MPa). A similar shift of T_g to 10°C was also observed with the MAPP treated composites, which implied efficient fiber matrix interfacial adhesion. However, the loss modulus value (8.09E + 07 MPa) at this temperature showed a decrease to 4%, thereby indicating the presence of a genuine interface.[29] The high temperature α relaxation peak of virgin PP also showed a comparative increase, to about 60°C and 67°C in the untreated and treated composites, respectively. In the matrix polymer, however, there was virtually no sharp inflection point of this process. Conversely, the filled composites displayed an increase in peak height and broadening of the relaxation region. This behavior is probably due to inhibition of the relaxation process, resulting in the decrease in the mobility of polymer chains in the crystallites.[30]

Loss tangent (tan δ)

The variation of tan δ as a function of temperature is illustrated in Figure 10. The damping peak in the treated composites showed a decreased magnitude of tan δ and broadening of the PP transition region in comparison to virgin PP and untreated composites.

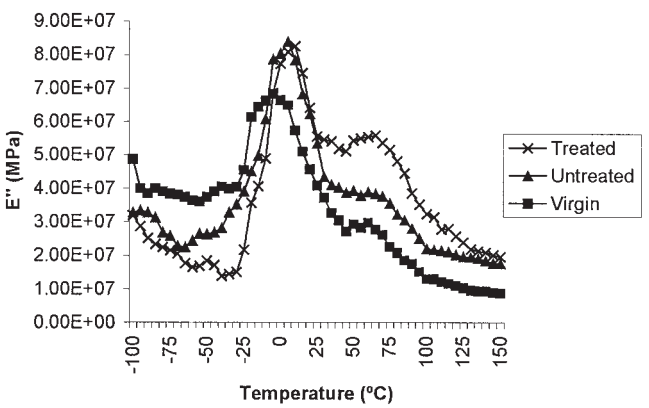

Figure 9 Variation of loss modulus of virgin PP and untreated and treated sisal–PP composites as a function of temperature.

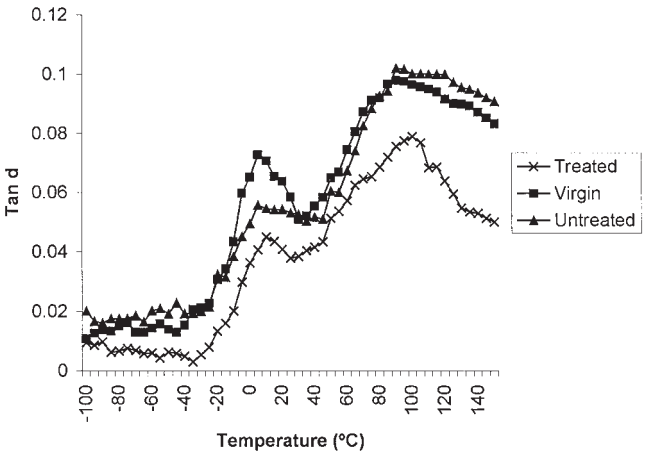

Figure 10 Variation of tan δ of virgin PP and untreated and treated sisal–PP composites as a function of temperature.

This is mainly because the fibers carry a greater extent of stress and allow only a small part of it to strain the interface.[25] Therefore, energy dissipation will occur in the polymer matrix and at the interface, with a stronger interface characterized by less energy dissipation.[31,32] This fact is substantiated in our experimental results, which further revealed efficient fiber matrix adhesion with the addition of MAPP. The untreated composites exhibited lower tan δ values in the glass transition region between –25 to 30°C due to fiber reinforcement that leads to less energy dissipation. However, at the other temperature regions, the values remained the same as the virgin matrix, which is indicative of poor fiber matrix interfacial bonding and ease of fibrillation of fibers.

CONCLUSION

The mechanical and dynamic mechanical properties of PP–sisal fiber composites have been investigated. It was observed that the composites prepared at 21 volume percent of fiber loading with 1% MAPP concentration showed optimum mechanical strength. Storage modulus versus temperature plots showed an increase in the magnitude of the peaks with the addition of fibers and MAPP. The damping properties of the composites, however, decreased with the addition of the fibers and MAPP. Based on these studies, it can be concluded that sisal fibers could reinforce the PP matrix when used in optimal concentration of fibers and coupling agents.

References

1. Coutinho, F. M. B; Costa, T. H. S.; Carvalho, D. L. J Appl Polym Sci 1997, 65, 1227.
2. Schneider, J. P.; Karmaker, A. C. ANTEC, 1995, 2086.
3. Mishra, H. K.; Dash, B. N.; Tripathy, S. S.; Padhi, B. N. Polym Plast Technol Eng 2000, 39, 187.

4. Mohanty, A. K; Khan, M. A; Hinrichsen, G. Composites: Part A 1999, 31, 143.
5. Tripathy, S. S.; DI landro, L.; Fontanelli, D.; Marchetti, A.; Levita, G. J Appl Polym Sci 2000, 75, 1585.
6. Rout, J.; Mishra, M.; Tripathy, S. S.; Nayak, S. K.; Mohanty, A. K. Polym Composites 2001, 22, 770.
7. Mishra, S.; Mishra, M.; Tripathy, S. S.; Nayak, S. K.; Mohanty, A. K. J Reinforced Plastics and Composites 2001, 20, 321.
8. Botev, M.; Betchev, H.; Bikaris D.; Panayiotou, C. J Appl Polym Sci 1999, 74, 523.
9. Mishra, S.; Mishra, M.; Tripathy, S. S.; Nayak, S. K.; Mohanty, A. K. Macrol Mater Eng 2001, 1, 286.
10. Mohanty, S.; Nayak, S. K.; Verma, S. K.; Tripathy, S. S. J Reinforced Plastics and Composites 2004, 23, 625.
11. Karmakar, A. C.; Youngquist, J. A. J Appl Polym Sci 1996, 62, 1147.
12. Ali, A. A.; Khan, M. A.; Ali, K. M. I.; Kinrichsen, G. J Appl Polym Sci 1998, 70, 843.
13. Dash, B. N.; Rana, A. K.; Mishra, H. K.; Nayak, S. K.; Mishra, S. C.; Tripathy, S. S. Polym Compos 1999, 20, 62.
14. Karmakar, A. C.; Hoffmann, A.; Hinrichen, G. J Appl Polym Sci 1994, 54, 1803.
15. Thwe, M. M.; Liao, K. J Mater Sci Letters 2003, 38, 363.
16. Cantero, G.; Arbelaiz, A.; Mugika, F.; Valea, A.; Mondragon, I. J Reinforced Plastics and Composites 2001, 22, 321.
17. Rout, J.; Mishra, M.; Nayak, S. K.; Tripathy, S. S.; Mohanty, A. K; Verma, S. K. Inter J Plastics Tech 2002, 5, 55.
18. Gassan, J.; Bledki, A. K. Polym Compos 1997, 13, 179.
19. Felix, J. M.; Gatenholm, P. J Appl Polym Sci 1991, 42, 609.
20. Rana, A. K.; Mandal, A.; Mitra, B. C.; Jacobson, R.; Rowell, R.; Banerjee, A. N. J Appl Polym Sci 1998, 69, 329.
21. Dong, S.; Sapieha, S.; Schreiber, H. P. Polym Engg Sci 1993, 33, 343.
22. Mieck, K. P.; Nechwatal, A.; Knobelsdorf, C. A. Makromole Chem 1995, 37, 225.
23. Joseph, P. V.; Rabello, M. S.; Mattaso, L. H. C.; Joseph, K.; Thomas, S. Compos Sci and Technol 2002, 62, 1357.
24. Xie, X. L.; Fung, K. L; Li, R. K. Y; Tjong, S. C; Mai, Y. W J Polym Sci: Part B: Polym Physics 2002, 40, 1214.
25. George, J.; Bhagawan, S. S.; Thomas, S. J Thermal Analysis 1996, 47, 1121.
26. Chu, N. J. J Appl Polym Sci 1998, 14, 3129.
27. George, J.; Bhagawan, S. S.; Thomas, S. J Thermal Analysis 1996, 47, 1121.
28. Saha, A. K.; Das, S.; Bhatta, D.; Mitra, B. C. J Appl Polym Sci 1998, 71, 1505.
29. Calleja, R. D.; Ribelles, J. L. G.; Pradas, M. M.; Greus, A. R.; Colomer, F. R. Polym Compos 1991, 12, 6.
30. Hashmi, S. A. R; Kitano, T.; Chand, N. Polym Compos 2003, 24, 149.
31. Suprapakorn, N.; Dhamrongvaraporn, S.; Ishida, H. Polymer Composites 2001, 19, 2.
32. Kim, J. I.; Ryu, S. H.; Chang, Y. W. J Appl Polym Sci 2000, 77, 2595.